Molecular Biology of the Cell
Vol. 15, 721–733, February 2004

Endocytosed Cation-Independent Mannose 6-Phosphate Receptor Traffics via the Endocytic Recycling Compartment en Route to the *trans*-Golgi Network and a Subpopulation of Late Endosomes

Sharron X. Lin,* William G. Mallet,*† Amy Y. Huang, and Frederick R. Maxfield‡

Department of Biochemistry, Weill Medical College of Cornell University, New York, New York 10021

Submitted July 16, 2003; Revised September 26, 2003; Accepted September 27, 2003
Monitoring Editor: Suzanne Pfeffer

Although the distribution of the cation-independent mannose 6-phosphate receptor (CI-MPR) has been well studied, its intracellular itinerary and trafficking kinetics remain uncertain. In this report, we describe the endocytic trafficking and steady-state localization of a chimeric form of the CI-MPR containing the ecto-domain of the bovine CI-MPR and the murine transmembrane and cytoplasmic domains expressed in a CHO cell line. Detailed confocal microscopy analysis revealed that internalized chimeric CI-MPR overlaps almost completely with the endogenous CI-MPR but only partially with individual markers for the *trans*-Golgi network or other endosomal compartments. After endocytosis, the chimeric receptor first enters sorting endosomes, and it then accumulates in the endocytic recycling compartment. A large fraction of the receptors return to the plasma membrane, but some are delivered to the *trans*-Golgi network and/or late endosomes. Over the course of an hour, the endocytosed receptors achieve their steady-state distribution. Importantly, the receptor does not start to colocalize with late endosomal markers until after it has passed through the endocytic recycling compartment. In CHO cells, only a small fraction of the receptor is ever detected in endosomes bearing substrates destined for lysosomes (kinetically defined late endosomes). These data demonstrate that CI-MPR takes a complex route that involves multiple sorting steps in both early and late endosomes.

INTRODUCTION

Proteins internalized from the plasma membrane may be sorted to several destinations, including degradative lysosomes, the *trans*-Golgi network (TGN), and the recycling pathways for return to the plasma membrane (Mukherjee *et al*., 1997). After endocytosis from the plasma membrane, proteins first enter sorting endosomes. From this compartment, some transmembrane proteins such as the transferrin receptor are delivered to the endocytic recycling compartment (ERC). Some transmembrane proteins (e.g., the epidermal growth factor receptor) and most soluble contents (e.g., low-density lipoprotein [LDL] released from its receptor) remain with sorting endosomes, which subsequently undergo a series of changes ("maturation") to become late endosomes (Dunn and Maxfield, 1992). The predominant pathway exiting the recycling compartment is transport back to the plasma membrane. From late endosomes, most substrates are delivered to lysosomes. However, alternative pathways have been described for several proteins.

We described previously the differential trafficking of two transmembrane proteins that are localized to the TGN, TGN38 (Ghosh *et al*., 1998) and furin (Mallet and Maxfield, 1999). After internalization, both eventually accumulate in the TGN, but furin is transported via late endosomes, whereas TGN38 transits through the endocytic recycling pathway. The selective sorting of these proteins at various steps depends upon specific amino acid sequences in their cytoplasmic domains that are recognized by cytosolic sorting factors (Humphrey *et al*., 1993; Ponnambalam *et al*., 1994; Voorhees *et al*., 1995).

A third example of an endocytosed protein that must undergo sorting away from the degradative and recycling pathways is the cation-independent mannose 6-phosphate receptor (CI-MPR), which transports lysosomal hydrolases to lysosomes via its recognition of phosphomannose modifications on the ligands (Dahms *et al*., 1989; Kornfeld, 1989). The CI-MPR transports newly synthesized enzymes from the TGN to acidic late endosomes, where the ligands dissociate, allowing the return of the CI-MPR to the TGN. Several recent studies have shown that GGA proteins associated with tubular structures are involved in trafficking between the TGN and late endosomes (Puertollano *et al*., 2001; Zhu *et al*., 2001; Doray *et al*., 2002; Ghosh and Kornfeld, 2003). Because the CI-MPR has a $t_{1/2}$ of 16 h in Chinese hamster ovary (CHO) cells (Sahagian and Neufeld, 1983), it must avoid prolonged residence in hydrolytically active late endosomes and lysosomes. A fraction of the CI-MPR is in the plasma membrane, where it binds to and internalizes ligands for delivery to lysosomes. Receptors internalized from the plasma membrane are eventually delivered to the TGN and distributed into the steady-state pattern, so the CI-MPRs are functionally in a single pool (Duncan and Kornfeld, 1988; Jin *et al*., 1989).

Article published online ahead of print. Mol. Biol. Cell 10.1091/mbc.E03–07–0497. Article and publication date are available at www.molbiolcell.org/cgi/doi/10.1091/mbc.E03–07–0497.

* These authors contributed equally to this work.
† Present address: Department of Molecular Oncology, Genentech, Inc., 1 DNA Way, MS 42, South San Francisco, CA 94080.
‡ Corresponding author. E-mail address: frmaxfie@med.cornell.edu.

The CI-MPR is detected in endosomes, in the TGN, and at the plasma membrane in varying proportions in different cell types (Willingham *et al*., 1983; Geuze *et al*., 1984; Griffiths *et al*., 1988; Press *et al*., 1998). The CI-MPR has been used as a marker for late endosomes due to its detection there by biochemical and ultrastructural methods (Goda and Pfeffer, 1988; Griffiths *et al*., 1988). However, work in HEp2 cells has shown that in those cells the receptor is relatively depleted from structures bearing the morphological and functional characteristics of late endosomes (Hirst *et al*., 1998), instead residing in distinct structures near the TGN. Also, CI-MPR accumulates in multivesicular structures that precede late endosomes on the degradative pathway in variant CHO cells that are deficient in degradation (Ohashi *et al*., 2000; Miwako *et al*., 2001). In CHO cells, some of the receptors colocalize with internalized α2-macroglobulin (α2M) after 4 min of α2M uptake, at which point the α2M would not have advanced far along the degradative pathway (Willingham *et al*., 1983). Recently, green fluorescent protein (GFP)-CI-MPR was detected in transferrin-positive endosomes in HeLa cells (Waguri *et al*., 2003). Similar results were obtained when the CI-MPR was compared with the recycling molecule transferrin (Tf) in NRK cells (Geuze *et al*., 1984).

The route that the receptor takes after endocytosis has been proposed to be from the plasma membrane to sorting endosomes, then to late endosomes, and finally to the TGN, which is similar to the path taken by furin (Dahms *et al*., 1989). However, the complete endosomal itinerary of the CI-MPR has not been evaluated in detail. Given the many transport pathways available in endosomes, the eventual destination cannot define a pathway, as illustrated by the examples of TGN38 and furin (Ghosh *et al*., 1998; Mallet and Maxfield, 1999). In this study, we set out to describe the steady-state distribution of the CI-MPR and more importantly to determine by what route the receptor achieves this distribution after endocytosis. To characterize CI-MPR trafficking pathways, CHO cells were transfected with a chimeric CI-MPR containing the bovine ecto-domain and the mouse transmembrane and cytoplasmic domains. By using monoclonal antibodies that specifically recognize the bovine ecto-domain of the chimeric CI-MPR, detailed kinetic analyses showed that the receptor passes through the endocytic recycling pathway before achieving its steady-state distribution in CHO cells. A model for the trafficking of CI-MPR in CHO cells is presented (see Figure 10).

MATERIALS AND METHODS

Antibodies and Reagents

A chimeric construct, encoding the bovine ectodomain and the murine cytoplasmic and transmembrane domains of the CI-MPR, inserted into pSFFVneo (Chen *et al*., 1997) was provided by Peter Lobel (Rutgers University, Piscataway, NJ). Two monoclonal antibodies, clones 86f7 and 32g, against the bovine ectodomain of the CI-MPR, were provided by Donald Messner (Pacific Northwest Medical Center, Seattle, WA) (Chen *et al*., 1993). Fab fragments were generated from 86f7 by using the ImmunoPure kit from Pierce Chemical (Rockford, IL). Antibodies and Fab fragments were conjugated to fluorescent dyes Alexa488 (Molecular Probes, Eugene, OR) and Cy3 (Jackson ImmunoResearch Laboratories, West Grove, PA) according to manufacturers' instructions. Antibody 86f7 was radio-iodinated as described previously (Yamashiro *et al*., 1989). Polyclonal antibodies against the CI-MPR were provided by Peter Lobel (Chen *et al*., 1993). Monoclonal antibody (mAb) AE/1 (against AP1) was provided by Linton Traub (Washington University, St. Louis, MO) (Traub *et al*., 1993). Polyclonal antibodies against furin were provided by Yukio Ikehara (Fukuoka University, Fukuoka, Japan) (Misumi *et al*., 1991). Polyclonal antibodies against TGN38 were provided by George Banting (University of Bristol, Bristol, United Kingdom) (Wilde *et al*., 1992). Polyclonal antibodies against AP3 were provided by Juan Bonifacino (National Institutes of Health, Bethesda, MD). mAb UH3 against LAMP-2 (Uthayakumar and Granger, 1995) was purchased from The Developmental Studies Hybridoma Bank (University of Iowa, Iowa City, IA) and conjugated to Cy3 or Alexa488. Polyclonal antibodies against β-COP were purchased from Affinity Bioreagents (Golden, CO). mAb against FLAG-tag was purchased from Sigma-Aldrich (St. Louis, MO). 6-{(*N*-[7-Nitrobenz-2-oxa-1,3-diazol-4-yl]amino)-hexanoyl}sphingosine, (C_6-NBD-ceramide), rhodamine-dextran (70,000 Da), and polyclonal antibodies against Alexa488 were purchased from Molecular Probes. Human apotransferrin (Sigma-Aldrich) was loaded with iron and labeled as described previously (Yamashiro *et al*., 1984). Low-density lipoproteins (LDL) were prepared and labeled as described previously (Pitas *et al*., 1981). Fluorescently labeled polyclonal antibodies against rabbit immunoglobulins were purchased from Jackson ImmunoResearch Laboratories.

Cell Culture

TRVb-1 cells are a CHO variant cell line that lacks endogenous transferrin receptors but stably expresses the human transferrin receptor (McGraw *et al*., 1987). TRVb-1 cells were transfected with the plasmids pSFFVneo/MPR and pMEP (encoding a hygromycin resistance gene) by using LipofectAMINE (Invitrogen, Carlsbad, CA). Cells expressing the chimeric receptor were selected in Ham's F-12 medium supplemented with sodium bicarbonate, penicillin/streptomycin, and 5% fetal bovine serum with 400 μg/ml G-418 and 200 U/ml hygromycin. Clonal populations were obtained by colony selection followed by limiting dilutions. Clonal cell lines were propagated in the presence of 100 U/ml hygromycin. For testing the effect of mutant mRme-1 G429R on CI-MPR endocytosis and recycling, TRVb-1 cells stably expressing chimeric CI-MPR were transiently transfected with cDNA of FLAG-epitope-tagged mRme-1 G429R (FLAG-mRme-1 G429R) (Lin *et al*., 2001).

Fluorescence Staining Methods

For microscopy, cells were grown to subconfluence on poly-D-lysine–treated number 1 coverslips affixed beneath holes cut into the bottom of 35-mm dishes. For incubations of live cells with antibodies or ligands, cells were treated as described previously (Mallet and Maxfield, 1999) except as indicated. Briefly, unless otherwise stated, cells were incubated with fluorescent probes, washed, and subjected to chases in McCoy's 5A medium (Invitrogen) supplemented with 2.2 g/l $NaHCO_3$, 20 mM HEPES, and 0.2% (wt/vol) bovine serum albumin (Sigma-Aldrich) at 37°C. For brief incubations and washes, cells were placed on a 37°C slide warmer. For longer intervals, cells were placed in a 37°C incubator under an atmosphere of 5% CO_2. Immediately before fixation, cells were washed rapidly with medium 1 (150 mM NaCl, 20 mM HEPES, 1 mM Ca_2Cl, 5 mM KCl, 1 mM $MgCl_2$, pH 7.4) at room temperature. Cells were then fixed with 4% paraformaldehyde in medium 1 for 10 min at room temperature. For indirect immunofluorescence labeling, fixed cells were permeabilized with 0.01% (wt/vol) saponin (Sigma-Aldrich) in medium 1 with 0.5% bovine serum albumin (AB buffer). Antibodies were diluted into AB buffer for application to cells, and all washes were with AB buffer. Labeling with NBD-C_6-ceramide (Pagano *et al*., 1989) was performed as described previously (Ghosh *et al*., 1998).

Microscopy

Fluorescence staining and microscopy were performed as described previously (Ghosh *et al*., 1998) by using either a Leica DMIRB inverted microscope equipped with a 63× 1.32 numerical aperture plan Apochromat objective or a Zeiss Axiovert 100M inverted confocal microscope equipped with an LSM 510 laser scanning unit and a 63× 1.4 numerical aperture plan Apochromat objective. Excitation on the LSM 510 U was with a 25-mW argon laser emitting at 488 nm, a 1.0-mW helium/neon laser emitting at 543 nm, and a 5.0-mW helium/neon laser emitting at 633 nm; emissions were collected using a 505- to 530-nm band-pass filter to collect Alexa 488 emissions and a 560- to 615-nm band-pass filter to collect rhodamine, Cy3, and DiI emissions, and a 650-nm-long-pass filter to collect Cy5 emissions.

General Experimental Procedures

Transport rates, overall expression levels, and cell surface expression were determined using anti-bCI-MPR antibodies conjugated to fluorescent tags or ^{125}I as described previously (Mallet and Maxfield, 1999). Specific experimental conditions are described in RESULTS and figure legends. Anti-bCI-MPR antibodies were typically applied at 5 μg/ml for live cell incubations. Fluorescent transferrin was used at 5 μg/ml and fluorescent LDL at 20 μg/ml. Polyclonal antibodies were used at 1–2 μg/ml. Labeling with antibody AE/1 against AP1 was performed after cell fixation with Bouin's reagent (Sigma-Aldrich); otherwise, cells were fixed with 4% paraformaldehyde. Endocytic recycling of CI-MPR was measured by incubating cells for 3 min with Alexa488-anti-bCI-MPR antibodies, then fixing the cells and incubating with anti-Alexa488 antibodies or incubating the cells for 2, 5, 10, 15, or 20 min in the absence or presence of anti-Alexa488 antibodies before fixation. No loss of cell-associated fluorescence was detected in the absence of anti-Alexa488 antibodies. The efficiency of Alexa488 fluorescence quenching by anti-Alexa488 (92%) antibody was estimated from the extent of quenching of cells incubated with Alexa488-anti-bCI-MPR antibodies on ice.

Image Processing

Processing of digitized images was performed using the MetaMorph image processing software package (Universal Imaging, Molecular Devices, Sunnyvale, CA). Images were corrected for background fluorescence and cross-over of signal between channels. Quantitative imaging was performed using typically 10 fields of ~20 cells per field for each data point. For quantitative microscopic analyses and ^{125}I-antibody experiments, data were fit using the SigmaPlot software program (SPSS Science, Chicago, IL).

Regional Correlation Coefficient Analysis

To quantify the extent of colocalization of different molecules with CI-MPR, we carried out a quantitative analysis to measure the r between the intensity levels in two images. Because the CI-MPR is in many places throughout the cell, we restricted the measurement of colocalization to the region surrounding an organelle of interest. We developed a method, using MetaMorph software, to automatically identify the region surrounding the organelle of interest in each cell and then to measure the r between pixel intensity values in two images within that region. We called this a regional r. First, images of the organelle markers (transferrin for the ERC or TGN38 for the TGN) were thresholded to define the fluorescent probe-labeled regions of interest. The outlines of the structures above the threshold were eroded by 6 pixels to eliminate small objects and then dilated by 20 pixels to include the labeled organelle and the surrounding region. Each pixel was 0.14 × 0.14 μm. These regions were then used as a mask of the second fluorescent channel for the r measurement. Correlation coefficients can range from −1 to +1; a higher regional r value indicates greater codistribution of two probes.

RESULTS

The Chimeric CI-MPR Colocalizes with the Endogenous CI-MPR and Partially Colocalizes with Various Intracellular Marker Proteins

Incubation of live cells with monoclonal antibodies against the ectodomain of the protein of interest has proven to be a valuable strategy for the analysis of endocytic trafficking. We expressed in CHO cells a chimeric form of the CI-MPR that incorporates the bovine ectodomain and the murine cytoplasmic and transmembrane domains of the receptor. Using well-characterized antibodies against the ectodomain of the bovine CI-MPR (anti-bCI-MPR) (Chen *et al*., 1993; Messner, 1993), we were able to follow the trafficking of the chimeric protein without an interfering signal from the endogenous hamster receptor. Two monoclonal antibodies, clones 86f7 and 32g, were used and did not differ in trafficking or distribution in the experiments we describe below. The chimeric receptor was shown previously to transport lysosomal enzymes to lysosomes, indicating that it is a functional equivalent to the native CI-MPR (Chen *et al*., 1997).

Because the trafficking of a protein must account for its distribution at steady state, our first objective was to investigate the steady-state distribution of the CI-MPR in our transfected CHO cell line. When fixed cells were immunolabeled with a mAb against the bovine receptor and polyclonal antibodies that recognize both the endogenous and exogenous proteins, the chimeric receptor distribution was seen to overlap almost perfectly with the overall receptor pattern (Figure 1A). The chimera was detected in a perinuclear concentration and in punctate structures extending to the cell periphery. This demonstrates that the expressed protein distributes as the endogenous protein does, allowing us to study CI-MPR trafficking by using the chimera. Most of the data presented in this report are from a single clonal cell line, with preliminary experiments performed with mixed cell populations. We observed no differences in uptake or distribution of the chimeric receptor as a function of expression level in the mixed population (our unpublished data).

We compared the distribution of the chimeric receptor with other markers for endocytic organelles and the Golgi, and at the most, only partial overlap was found with any of the other proteins examined. Specifically, the distribution of the receptor in fixed cells coincided partially with that of the

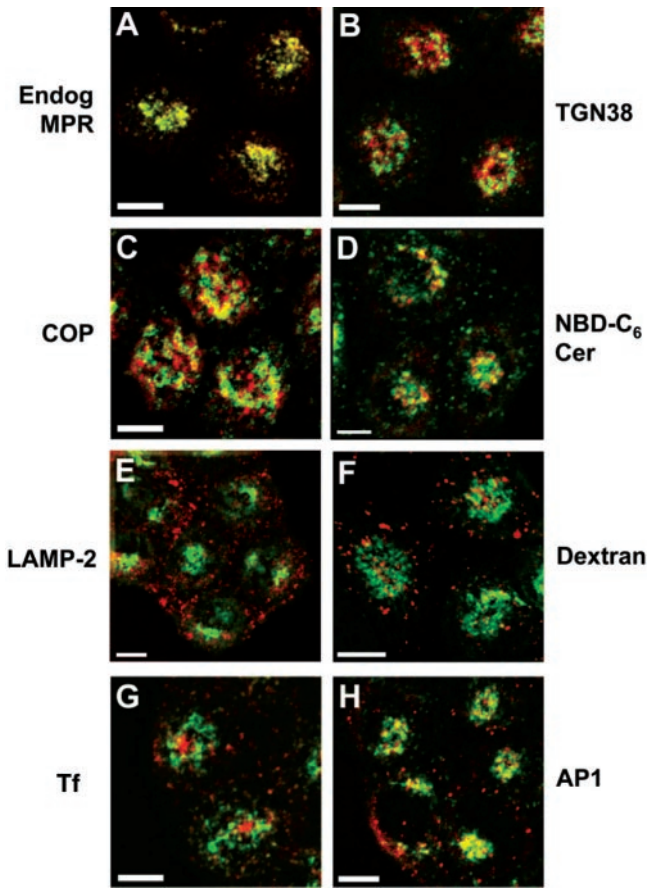

Figure 1. At steady state, the chimeric CI-MPR completely codistributes with endogenous CI-MPR and localizes to endosomes and the TGN/Golgi. TRVb-1 cells were fixed, permeabilized, and labeled with Alexa488-anti-bCI-MPR and polyclonal antibodies against endogenous CI-MPR (A, Endog MPR), TGN38 (B), β-COP (C, COP), and LAMP-2 (E), followed by Cy3-anti-rabbit secondary antibodies. In F, TRVb-1 cells were incubated with 10 mg/ml rhodamine-dextran (70 kDa, fixable) for 60 min, which labels mostly late endosomes and lysosomes, and then fixed. TRVb-1 cells expressing the CI-MPR chimera were incubated for 60 min with Cy3-transferrin (G) or with Cy3-anti-bCI-MPR for 2 h (D and H). The cells that received the anti-MPR in the medium were fixed and labeled with C_6-NBD-ceramide (D, NBD-C_6 Cer) to mark the TGN or with antibodies against the clathrin adaptor AP1 (H). Shown are confocal Z-series projections. For simplicity, chimeric MPR is pseudocolored in green in all panels. Bars, 5 μm.

TGN markers TGN38 (Luzio *et al*., 1990) (Figure 1B) and furin (Bosshart *et al*., 1994) (our unpublished data) and the Golgi marker β-COP (Duden *et al*., 1991) (Figure 1C). To examine the localization of the CI-MPR further in relation to the TGN, we used another *trans*-Golgi marker: the vital dye C_6-NBD-ceramide (Pagano *et al*., 1989). Staining with this dye cannot be performed in detergent-permeabilized cells, so we could not perform the receptor localization as for the other samples. As we show below, anti-bovine CI-MPR antibodies bound to the receptors on the cell surface rapidly achieve their steady-state distribution. Therefore, cells were incubated with anti-bovine CI-MPR antibodies for 2 h, fixed, and stained with C_6-NBD-ceramide (Figure 1D). Again, a partial colocalization of the chimeric CI-MPR with this TGN marker was observed in the perinuclear region of the cells.

The second expected site of localization of the CI-MPR is late endosomes, based on the function of the receptor and a

variety of morphological and biochemical studies. The CI-MPR itself is often used as a defining marker for late endosomes, but such studies rarely address, in quantitative terms, what proportion of the CI-MPR is in late endosomes. One protein that is found in late endosomes is the lysosomal membrane protein LAMP-2 (Lippincott-Schwartz and Fambrough, 1987; Uthayakumar and Granger, 1995). We detected little colocalization of LAMP-2 with the chimeric CI-MPR (Figure 1E), and similar data were obtained using endocytosed dextran, which labels mostly late endosomes and lysosomes after a 60-min incubation (Ghosh *et al*., 1998) (Figure 1F). We also found that most of the late endosomes labeled with an antibody against lysobisphosphatidic acid contained little of the endogenous CI-MPR (our unpublished data), as had been reported previously (Kobayashi *et al*., 1999). The segregation of most CI-MPR from LAMP-2 suggests that little CI-MPR enters lysosomes or that the epitope for the anti-MPR antibody is rapidly lost upon transport into lysosomes.

We found that the chimeric receptor colocalized partially with Tf in the sorting endosomes and in the ERC. Continuous incubation with fluorescent Tf results in labeling of the peripheral sorting endosomes (small dispersed spots in Figure 1G) and the ERC (large central structure in Figure 1G) (Hopkins and Trowbridge, 1983; Yamashiro *et al*., 1984). At steady state, although very little CI-MPR was found in the ERC, a minor but reproducible fraction of this receptor was detected in sorting endosomes (Figure 1G; note yellow-orange peripheral spots). Finally, the distribution of chimera CI-MPR was compared with AP1, a clathrin coat adaptor involved in vesicle transport out of the TGN (Hirst and Robinson, 1998). Recently, both AP1 and GGAs were shown to play important roles in mediating the transport of the CI-MPR from the TGN to the late endosomes (Puertollano *et al*., 2001; Zhu *et al*., 2001; Doray *et al*., 2002; Hinners and Tooze, 2003). As shown in Figure 1H, CI-MPR and AP1 overlapped partially in the vicinity of the TGN, but peripheral structures were labeled only with one or the other probe. The segregation of the two proteins in peripheral vesicles is consistent with the removal of AP1 from MPR-containing transport vesicles shortly after budding from the TGN, but it may also be that the AP1-labeled structures and the MPR-labeled structures arise from completely independent pathways. Essentially no colocalization was detected between the chimeric CI-MPR and the adaptor complex AP3 (Le Borgne *et al*., 1998) (our unpublished data), consistent with the proposed function of AP3 in vesicular transport (Dell'Angelica *et al*., 1998; Drake *et al*., 2000).

To exclude that the lack of extensive colocalization of the chimeric CI-MPR with late endosomal markers at steady state and the limited but persistent codistribution of CI-MPR with Tf are artifacts of the chimeric construct, we compared the steady-state distribution of the endogenous CI-MPR with other markers in cells not expressing the chimeric receptor (Figure 2). Endogenous CI-MPR overlapped significantly with Tf during a 5-min pulse labeling of Tf in sorting endosomes (Figures 2, A and B, arrows). When cells were incubated with Cy5-LDL over a pulse/chase time course and labeled for the endogenous CI-MPR after fixation, little colocalization of LDL with endogenous CI-MPR was observed after 10 or 20 min of chase (Figure 2, C and D). At these time points, LDL is mostly accumulated in maturing endosomes or late endosomes (Dunn and Maxfield, 1992). These results indicate that internalized LDL does not accumulate in a CI-MPR–enriched compartment before its degradation in late endosomes and lysosomes, which is consistent with the behavior observed for the chimeric receptor.

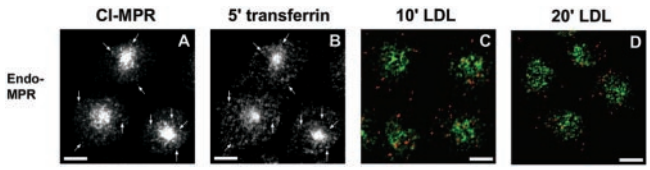

Figure 2. Endogenous hamster CI-MPR colocalizes partially with internalized Tf. TRVb-1 cells not expressing recombinant CI-MPR (A–D) were incubated for 5 min with 5 μg/ml Cy3-Tf (B, in A-B), and then fixed, permeabilized, and stained with 5 μg/ml Alexa488-anti-bCI-MPR (A). Arrows point to peripheral endosomes labeled for both molecules. Z series confocal projections are shown. In C and D, cells were incubated with 20 μg/ml Cy5-LDL for 5 min, and then washed and chased in medium for 10 or 20 min before fixation. Cells were then permeabilized and stained with anti-MPR antibody followed by Cy3-antirabbit secondary antibody. LDL is pseudocolored in red and MPR in green in both panels. Z-series confocal projections are shown. Bars, 5 μm.

Endocytosed CI-MPR Is Delivered to TGN via the Tf-positive ERC

Colocalization of the chimeric CI-MPR with Tf after pulse labeling and with Tf at steady state suggests that a significant portion of CI-MPR might traffic along part of the endocytic recycling pathway. To extend these observations, we coincubated cells with Cy3-anti-bCI-MPR antibody and Alexa488-Tf and then fixed and immunolocalized TGN38 with Cy5-secondary antibody in the same cells. To ensure that a sufficient amount of the anti-bCI-MPR antibodies was internalized into the cells for the detection of its accumulation in different organelles, we pulsed the cells with Cy3-anti-bCI-MPR antibodies for 30 min. As shown in Figure 3a (A–F), after 30 min of coincubation, CI-MPR colocalized extensively with Tf. At this time point, some colocalization of CI-MPR with TGN38 was also detected. These results suggest that the majority of the internalized CI-MPR enters the Tf-positive ERC before being delivered to the TGN. Interestingly, at this time, most of the CI-MPR was found in either the ERC or the TGN, as indicated by the small amount of red labeling in Figure 3D. When cells were chased without anti-bCI-MPR antibodies but with Tf in the chase medium for an additional 30 min, an increased colocalization of CI-MPR with TNG38 along with a decreased codistribution with Tf was detected (Figure 3a [G–L] and c). The extent of overlap of internalized CI-MPR with Tf and TGN38 was quantified using a regional r analysis, which measures the correlation of the intensity values in the two images. As illustrated in Figure 3, b and c, a higher regional r between CI-MPR, and Tf was observed in the absence of chase compared with the r after 30-min chase. In contrast, the regional r between internalized CI-MPR and TGN38 increased at longer chase times. These data further indicate the transient transport of internalized CI-MPR through the ERC before its accumulation in the TGN. After 30-min incubation followed by a 30-min chase, the chimeric CI-MPR has nearly reached its steady-state distribution. These data suggest that at steady state a significant amount of CI-MPR (both endogenous and chimeric) resides in either the TGN or the ERC, indicated by the small amount of red labeling shown in Figure 3J.

To investigate more directly the compartments that the chimeric CI-MPR transits through en route to its steady-state distribution, we next examined how internalized anti-bCI-MPR antibodies traffic during a brief incubation. In one procedure (Figure 4), we incubated cells for 5 min with Alexa488-anti-MPR antibodies and Cy5-Tf, and then fixed

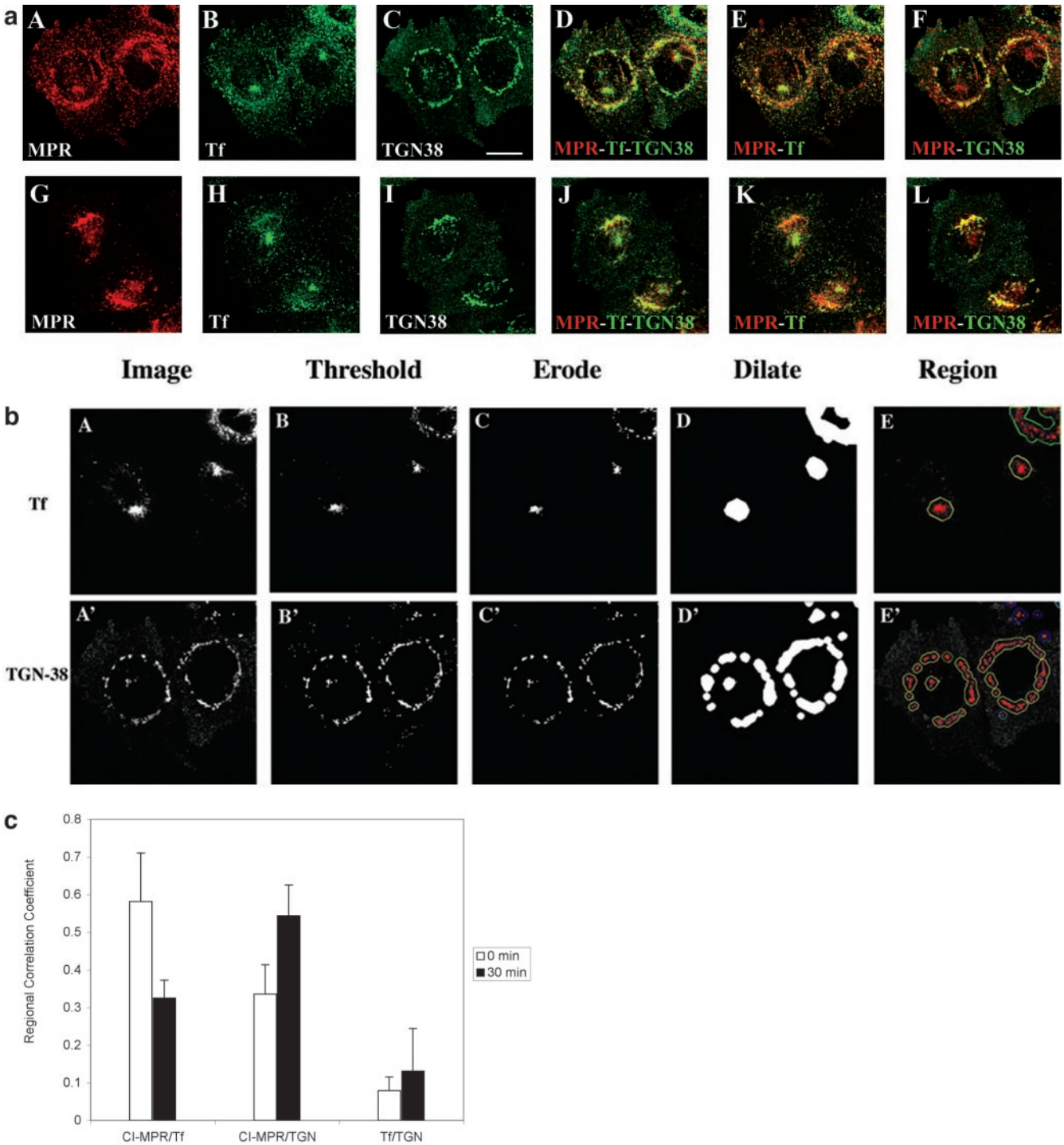

Figure 3. Most of the chimeric CI-MPR is found in the endocytic recycling compartment and the TGN. In a, TRVb-1 cells expressing the chimeric CI-MPR were incubated with Cy3-anti-bCI-MPR and Alexa488-Tf for 30 min (A–F) and followed by chase for 30 min (G–L) in the absence of Cy3-MPR but in the presence of Alexa488-Tf. Cells were then fixed, permeabilized, and stained with anti-TGN38 antibody, followed with Cy5-goat anti-rabbit secondary antibody (C and I). The Cy3-anti-bCI-MPR staining is shown in A and G, the Alexa488-Tf staining is shown in B and H and the TGN38 antibody staining is shown in C and I. For the convenience of direct comparison, TGN38 staining was pseudocolored in green. In D and J, the distribution of CI-MPR (red) was compared with that of both Tf and TGN38 (both are green). In E and F and K and L, the distribution of MPR (red) was compared with Tf (green in E and K) and TGN38 (green in F and L). Bars, 10 μm. In b, the method to generate the regions of interest for the measurement of regional r is illustrated. First, images of the organelle marker (transferrin or TGN38) were thresholded to define the fluorescent probe-labeled regions of interest. The thresholded objects were eroded by 6 pixels to eliminate small objects, and the remaining objects were dilated by 20 pixels to include the labeled organelle and the surrounding region. These regions were then used as a mask of the internalized CI-MPR channel for the r measurement. Results of these measurements and analysis based on seven images containing ~29 cells are shown in the Figure 3C.

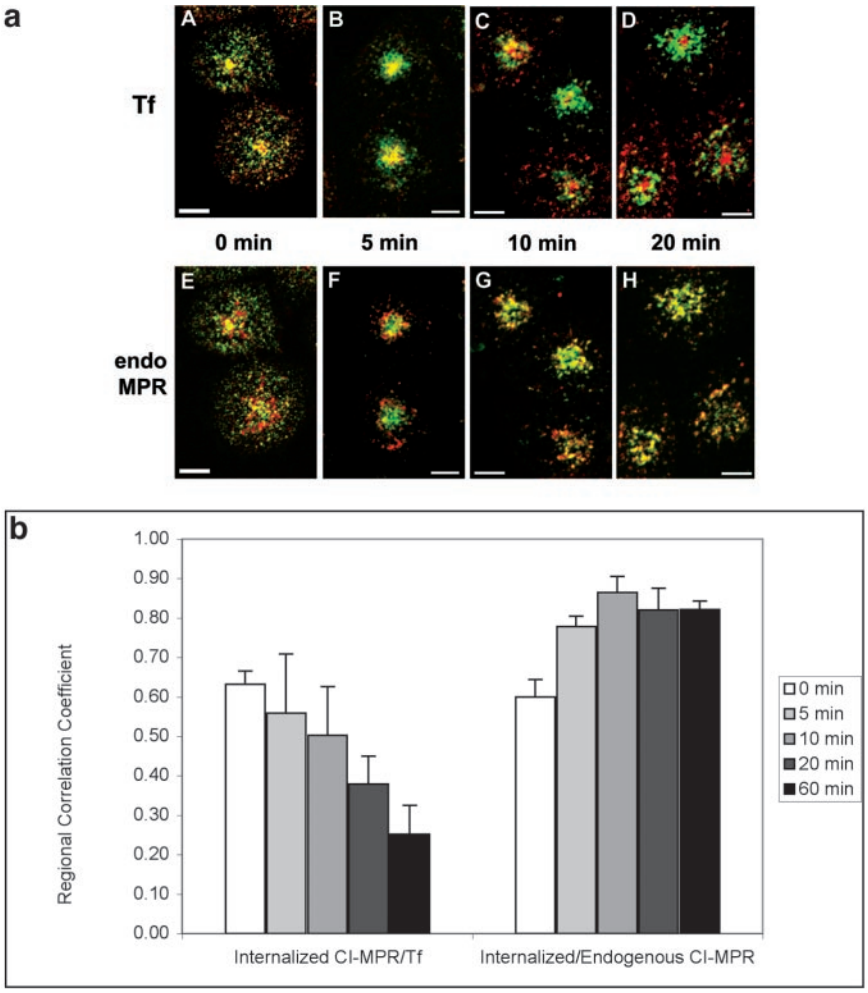

Figure 4. The chimeric CI-MPR enters the endocytic recycling compartment after internalization, and then rapidly exits the recycling pathway and reaches steady state. In a, cells were incubated for 5 min with Alexa488-anti-bCI-MPR and with Cy5-Tf (A–D) or without Cy5-Tf (E–H). Cells were then washed and fixed (A and E) or chased for 5, 10, and 20 min in medium containing Cy5-Tf (B–D) or without Cy5-Tf (F–H) before fixation. In E–H, cells were permeabilized and stained with antibodies against the endogenous CI-MPR followed by Cy3-labeled secondary antibodies. The chimeric CI-MPR is pseudocolored in green in all panels. Cy5-Tf is pseudocolored red in A–D; endogenous CI-MPR (endo MPR) is red in E–H. Z series confocal projections are shown. Bars, 5 μm. In b, the method illustrated in Figure 3B was used to generate the regions of interest for the measurement of regional r. First, images of the organelle marker (transferrin or endogenous CI-MPR) were thresholded to define the fluorescent probe-labeled regions of interest. The thresholded objects were eroded by 6 pixels to eliminate small objects, and the remaining objects were dilated by 20 pixels to include the labeled organelle and the surrounding region. These regions were then used as a mask of the internalized CI-MPR channel for the regional r measurement, which is based on the intensity values in the identical pixels in the two images. Results of these measurements and analysis based on 11 images containing ~47 cells are shown in the Figure 4b.

the cells or allowed the probes to be chased for various times before fixation. Fluorescent Tf (Figure 4, A–D) was included in the chase medium to prevent loss of this probe due to recycling. Cells were then immunolabeled with antibodies to the CI-MPR and Cy3-secondary antibodies (Figure 4, E–H). by using the same fields of triple labeled cells for comparisons, the distribution of the internalized chimeric receptor (pseudocolored in green) is compared with Tf (red, Figure 4, A–D) and with the endogenous receptor (red, Figure 4, E–H). In the absence of a chase, internalized CI-MPR colocalizes well with Tf, both in peripheral endosomes and in the juxta-nuclear ERC (Figure 4A). In addition, elements of colocalization with the steady-state distribution of the receptor can also be detected at this early stage of transport, particularly in punctate structures (Figure 4E). These observations hold with a 5-min chase (Figure 4, B and F), although the sorting endosome labeling of both Tf and the chimeric CI-MPR decreased during the chase, as expected. Typically, the CI-MPR labeling was somewhat more enriched in the punctate endosomes and the Tf more in the ERC. After a 10-min chase, however, the internalized receptor began to segregate from Tf and to accumulate in the pericentriolar pattern characteristic of its steady-state distribution (Figure 4C). Overlap with the endogenous receptor increased greatly at the same time (Figure 4G). By 20 min of chase, the internalized receptor seemed to be close to its steady-state distribution (Figure 4H), and colocalization with Tf was now restricted to a minor population of peripheral endosomes (Figure 4D). The degree of colocalization of the internalized CI-MPR with Tf and the endogenous CI-MPR was measured and quantified using regional r analysis. As shown in Figure 4b, after the initial 5-min uptake, the regional r between CI-MPR and Tf was found to decrease with longer chase time. In contrast, after the initial uptake, the regional r between internalized CI-MPR and endogenous CI-MPR increased during the chase. Interestingly, a further decrease in the value of the regional r was observed between internalized CI-MPR and Tf between 20- and 60-min chase (Figure 4b), indicating that longer time (>10- to 20-min chase) was needed for internalized CI-MPR to completely reach its steady-state distribution.

To verify the transport of chimeric CI-MPR through the ERC after endocytosis, a dominant-negative mutant of mRme-1 (flag-mRme-1 G429R) was expressed transiently in TRVb-1 cells stably expressing the chimeric receptor. Rme-1 (EHD1) is an Eps15-homology (EH) domain protein that is associated with the ERC. We have shown previously that expressing mRme-1 with a point mutation near the EH domain, G429R, slowed Tf recycling to the plasma membrane from the ERC as well as TGN38 transport from the ERC to the TGN (Lin *et al.*, 2001). If endocytosed anti-bCI-MPR antibody passes through the ERC before delivery to TGN, it should be trapped in the ERC in cells expressing mRme-1 G429R. We found, in cells expressing mRme-1

Table 1. Expressing mRme-1 G429R results in decreased MPR uptake

TRVb-1 cells stably transfected with chimeric MPR were transiently transfected with FLAG-mRme-1 G429R. Cells were incubated with Cy3-anti-bCI-MPR for 5 min followed by chase in the absence of Cy3-anti-bCI-MPR for 2.5 min or for 30 min. Data from a representative experiment are shown.

Cells	Experiment	% of CI-MPR uptake	No. of cells
Control	5-min uptake	100	23
mRme-1 G429R	5-min uptake	57	64
Control	2.5-min chase	100	11
mRme-1 G429R	2.5-min chase	56	40
Control	30-min chase	100	21
mRme-1 G429R	30-min chase	54	108

G429R, the CI-MPR internalization was reduced by about one-half (Table 1), which would be consistent with reduced surface expression of receptors due to impaired recycling. As shown in Figure 5, A–C, cells expressing mutant mRme-1 G429R (identified by retention of Tf; Figure 5A) showed a significant accumulation of CI-MPR in the ERC after a 30-min incubation with Cy3-anti-bCI-MPR antibody (Figure 5B). To compensate for the decreased amount of anti-bCI-MPR antibody internalized into cells expressing mutant mRme-1 G429R, the intensities of anti-bCI-MPR antibody staining in Figure 5, B and C, and E and F were scaled up to observe the accumulation and localization of anti-bCI-MPR antibody in these cells. As a result, cells not expressing mRme-1 G429R displayed a high intensity of CI-MPR labeling. For cells expressing mutant mRme-1 G429R, retention in the ERC was seen after a 30-min chase (Figure 5, D and E). At the same time points, in cells not expressing mRme-1 G429R (no retention of Tf), limited overlap of CI-MPR with Tf was observed (Figure 3K). These data provide additional evidence that CI-MPR traffics through the endocytic recycling compartment. Expression of mRme-1 G429R shows no effect on the delivery of DiI-LDL or dextran to late endosomes after internalization from the cell surface (Lin *et al.*, 2001).

CI-MPR Segregates Away from LDL after Cointernalization

After internalization from the plasma membrane, Tf-receptors are removed from sorting endosomes and delivered to the ERC, whereas probes destined for lysosomes (e.g., LDL) stay in the sorting endosomes as they mature into late endosomes (Salzman and Maxfield, 1989; Dunn and Maxfield, 1992). The delivery of the CI-MPR into sorting endosomes and the ERC suggests that it too may be sorted away from LDL after internalization. To examine this directly, cells were incubated for 5 min with DiI-labeled LDL and Alexa488-anti-MPR antibodies, and then fixed immediately or chased for up to 20 min (Figure 6). We found that internalized CI-MPR and LDL colocalized most extensively immediately after the 5-min pulse, when LDL is nearly all in sorting endosomes (Figure 6A). After a 5-min chase, only a minority of LDL-labeled endosomes contained detectable anti-bCI-MPR antibodies, and the segregation was nearly complete by 20 min of chase (Figure 6D). Note that the anti-bCI-MPR antibodies labeled small LDL-free structures at all time points. These data and the data in Figures 3–5 show that internalized CI-MPR initially follows the endocytic recycling pathway from the sorting endosomes to the ERC. However, the CI-MPR seems to maintain colocalization with LDL for longer than does Tf, indicating that the CI-MPR may not exit sorting endosomes at the same rate as the Tf-receptor.

Because many of the experiments described in this article followed the trafficking of monoclonal anti-bCI-MPR antibodies bound to the receptor, we investigated whether the antibodies could artifactually influence trafficking by antigen cross-linking or some other mechanism. The delivery of the labeled antibody to its steady-state sites by endocytosis demonstrates that addition of the antibody does not significantly alter the overall trafficking of the chimeric protein. We also found that the distributions of internalized anti-MPR IgG versus monovalent Fab fragments did not differ at any stage of their trafficking (our unpublished data). Finally, no change in the steady-state patterns of either the chimeric protein or the endogenous receptor was observed upon

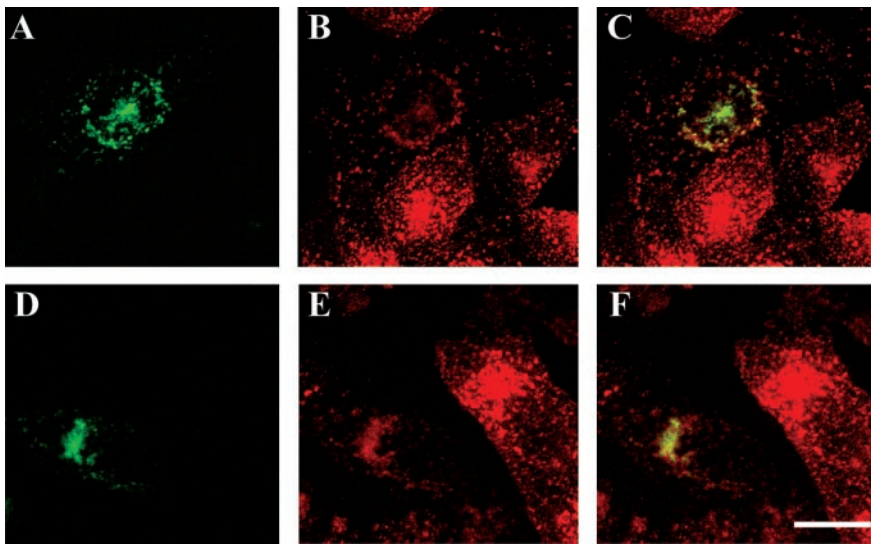

Figure 5. Expressing mutant mRme-1 G429R slows the exit of chimeric MPR from the ERC and decreases the receptor recycling to the cell surface. TRVb-1 cells stably transfected with chimeric CI-MPR were transiently transfected with FLAG-mRme-1 G429R. Cells were incubated with Cy3-anti-bCI-MPR for 30 min (A–C) followed by chased in the absence of Cy3-anti-bCI-MPR for an additional 30 min (D–F). In A–C, Alexa488-Tf (A) was preincubated with cells for 15 min and chased in the absence of Alexa488-Tf but in the presence of excess unlabeled Tf for 15 min before and during the incubation of Cy3-anti-bCI-MPR for 30 min (B). The total chase time for Tf is 45 min. In D–E, Alexa488-Tf (D) was incubated together with Cy3-anti-bCI-MPR (E) for 15 min and was chased for 45 min. The merged images of A and B and D and E are shown in C and F, respectively. Z series confocal projections are shown. Bars, 10 μm.

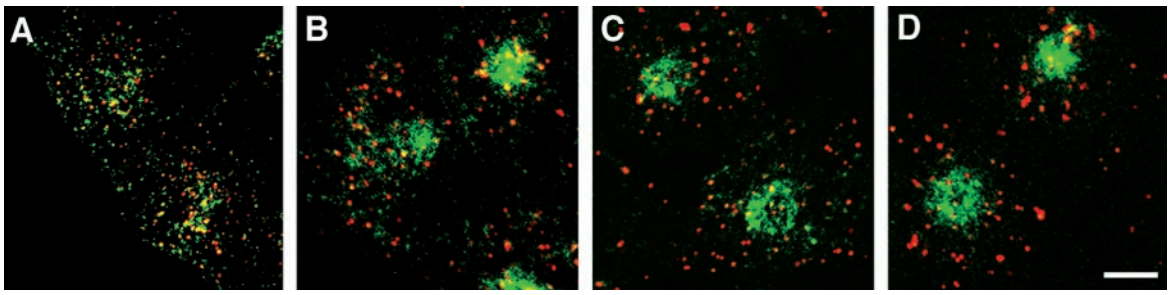

Figure 6. The chimeric CI-MPR showed limited codistribution with late endosomal probes. TRVb-1 cells expressing recombinant chimeric CI-MPR were incubated with 5 μg/ml Alexa488-anti-bCI-MPR (green) and 20 μg/ml DiI-LDL (red) for 5 min, and then were washed and fixed (A) or chased for 5 (B), 10 (C), or 20 (D) min before fixation. Shown are confocal Z-series projections. Bars, 5 μm.

adding antibodies to the culture medium (our unpublished data). Therefore, it is very likely that our observations reflect the trafficking of the unperturbed chimeric CI-MPR and are not influenced greatly by antibody binding.

Kinetics of Chimeric CI-MPR Trafficking

The appearance of internalized CI-MPR in the ERC suggests that at least a fraction of the protein may be recycled back to the plasma membrane with each round of internalization. To determine whether this is so, we used a technique that we used previously to measure the endocytic recycling of internalized TGN38 (Ghosh *et al.*, 1998). Cells were incubated with Alexa488-conjugated anti-bCI-MPR antibodies for 3 min, and then fixed or chased for 2–20 min with anti-Alexa488 antibodies in the chase medium. If the internalized receptor is recycled, it will be delivered to the plasma membrane where the Alexa488 fluorescence will be quenched by anti-Alexa488 antibody. We observed a rapid loss of cell-associated fluorescence during the chase (Figure 7A). After 2 min of chase, the anti-bCI-MPR antibody was detected in peripheral sorting endosomes and in the recycling compartment (Figure 7B), as also shown in Figures 4A and 6A. After 20-min chase, however, the cell-associated fluorescence was greatly diminished (Figure 7C). The rate of loss of fluorescence is a measure of the rate of endocytic recycling, and we calculate that the chimeric CI-MPR recycled with a half-time of 5–6 min. This is a rapid recycling rate compared with recycling via the ERC (McGraw and Maxfield, 1990; Mayor *et al.*, 1993; Ghosh *et al.*, 1998), which may indicate that some of the CI-MPR recycles by a faster direct route from the sorting endosomes to the plasma membrane (Hao and Maxfield, 2000). Correcting for the fact that anti-Alexa488 antibodies quenches with ~92% efficiency in this procedure, we estimate that ~84% of the internalized CI-MPR is rapidly recycled. The remainder is subsequently detected in a distribution indistinguishable from the steady-state pattern of the protein, as illustrated by a longer exposure of the 20-min quench field (Figure 7D) compared with a field of cells that did not receive anti-Alexa488 antibodies (Figure 7E). This suggests the existence of a mechanism that diverts some of the receptor from recycling to the plasma membrane and directs it to the TGN.

Despite the large flux of CI-MPR through the endocytic recycling pathway, very little receptor is detected in the recycling compartment at steady state. This could be explained by the rapid recycling of the protein from the ERC and by relatively slow efflux from the other compartments. We measured the overall rate of efflux of the chimeric protein from its steady-state distribution by three different methods. First, cells were incubated continuously for various times with radio-iodinated anti-bCI-MPR antibodies, and the accumulation of the antibodies in the cells was measured over time. The initial binding was ~10% of the maximal value, and this represents the fraction of receptors on the cell surface. The rate of the subsequent accumulation is the rate at which the protein exits its intracellular sites and occurs at the plasma membrane (Ghosh *et al.*, 1994). Note that the kinetics may be the result of multiple pathways, because the CI-MPR resides in several compartments at steady state. Using iodinated antibodies, we estimate that the half-time of efflux of the chimeric CI-MPR was ~40 min (Figure 8A). This rate was also measured by continuous incubation with fluorescent antibodies, yielding a half-time of ~27 min (Figure 8B). By either protocol the efflux of the protein from steady state is much slower than its endocytic recycling rate after a short filling pulse. To derive the externalization rate using a third approach, cells were incubated continuously with Alexa488-anti-bCI-MPR antibody for 60 min to allow the antibody to reach steady state, and then cells were incubated further with anti-Alexa488 antibodies in the medium. Under these conditions, the rate of loss of fluorescence is a measure of the overall rate of efflux from its steady-state distribution, and we measured this rate to have a half-time of 29 min (Figure 8C). The fact that the receptor bound to a fluorescent antibody exits the cell with a similar rate as unoccupied receptor further shows that antibody labeling is unlikely to alter the trafficking of the protein.

Radio-iodinated antibodies were also used to measure the rate of endocytosis of the CI-MPR, the level of plasma membrane expression, and the total expression level (Table 2). The protein is internalized with a half-time of 2.5 min, a typical rate for a transmembrane receptor (Figure 8D). At steady state, we detect ~11% of the chimeric receptor at the plasma membrane. The clonal line expresses ~6×10^5 chimeric receptors per cell. The rapid rates of endocytosis and recycling, coupled with the slow overall rate of efflux, allow the receptor to accumulate in a pericentriolar pattern, apparently over several rounds of uptake and transport.

Endocytosed CI-MPR Is Detected in Late Endosomes Subsequent to Accumulation in the Pericentriolar Region of the Cell

Many ultrastructural studies have detected the CI-MPR in late endosomes. Although the receptor leaves sorting endosomes before they mature into late endosomes, it must traffic to late endosomes subsequently to carry out its enzyme delivery function. To observe this delivery to late endosomes, we incubated cells for 30 min with fluorescent anti-bCI-MPR antibody, and then chased the antibodies into the cells for 90 min. During the end of this incubation, the cells

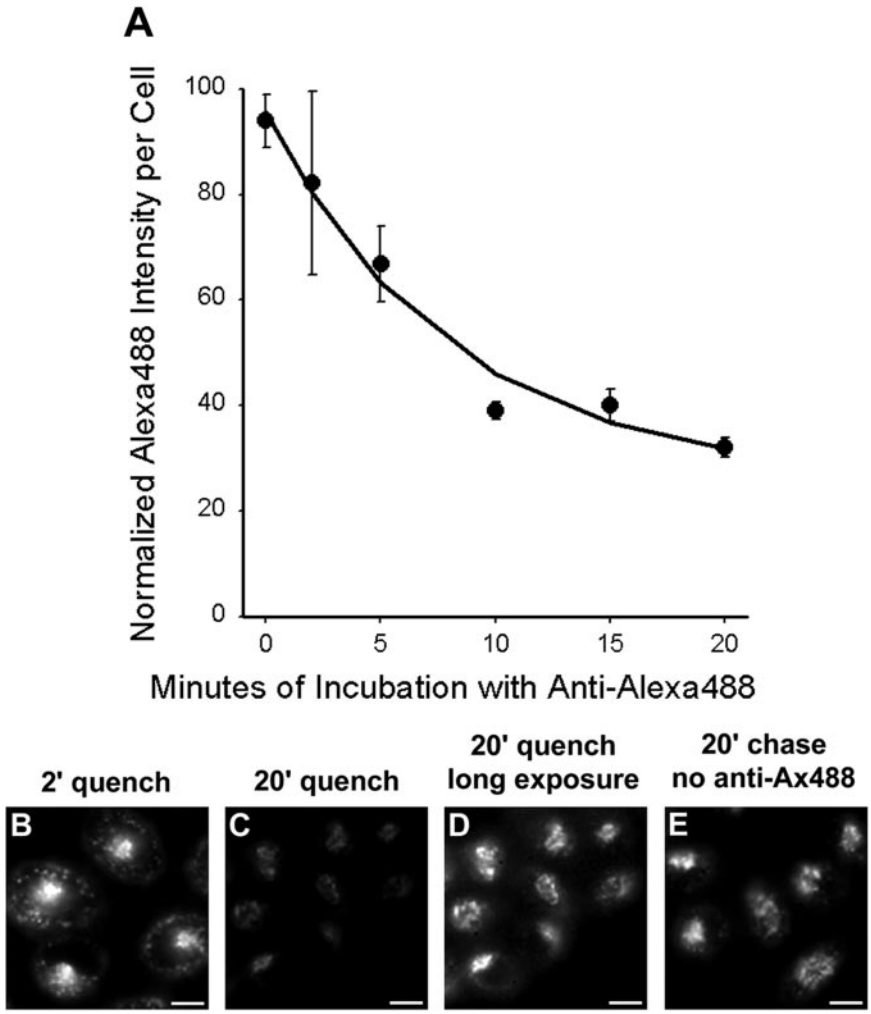

Figure 7. A substantial fraction of internalized CI-MPR is rapidly recycled to the plasma membrane through endosomes. (A) Cells were incubated for 3 min with 5 μg/ml Alexa488-anti-bCI-MPR, and then washed briefly. Cells were incubated with 10 μg/ml anti-Alexa488 for 2, 5, 10, 15, or 20 min before fixation. To obtain the zero-minute time point, cells were fixed after the Alexa488-anti-bCI-MPR pulse and incubated with anti-Alexa488 to quench antibody that had not yet been internalized. Unquenched fluorescence was detected by wide-field microscopy. Relative fluorescence intensities per cell are plotted as a function of time of incubation with anti-Alexa488. Data have been fitted to a mono-exponential decline. (B–E) Representative images from such an experiment, showing Alexa488 fluorescence after 2 min (B) or 20 min (C) with anti-Alexa488, or 20-min chase without anti-Alexa488 (E). (D) Enhanced copy of Panel C to illustrate the distribution of unquenched anti-bCI-MPR. Bars, 5 μm.

received DiI-LDL for 5 min with no chase or with chases of 10 or 30 min (Figure 9) before fixation. After 90 min, the CI-MPR should be in its steady-state distribution, and the LDL will be in various stages of transport along the degradative pathway, depending on the length of the LDL chase. This procedure differs from that used in Figure 6, in which both probes were introduced and chased simultaneously. In the absence of a chase, LDL was detected in dispersed sorting endosomes and very limited colocalization of LDL with CI-MPR in the sorting endosomes was observed at this time point (Figure 9A-C; arrows point to CI-MPR-positive spots that do not contain LDL). After 10 min of chase, much of the LDL should be in late endosomes or transitional maturing endosomes, and at this point colocalization of LDL with CI-MPR was substantially increased versus no chase (Figure 9, D–F; arrows indicate nonoverlapping spots and arrow heads indicate overlapping spots). A further increase in overlap of the two molecules was detected with a 30-min chase (Figure 9, G–I; arrowheads indicate overlapping spots). Still, the punctate structures labeled with both CI-MPR and LDL were much more intensely stained with DiI-LDL and represented a very small fraction of the total CI-MPR distribution. We did not extend this analysis beyond 30 min because DiI-LDL degrades at later times. After 10 min and 30 min of chase, endosomes labeled with internalized LDL no longer contain recycling molecules such as Tf (Dunn and Maxfield, 1992), so these endosomes are maturing endosomes or late endosomes by kinetic criteria. This result, along with data shown in Figure 6, suggests that detectable accumulation in kinetically defined late endosomes is a distal event in the trafficking of the CI-MPR.

DISCUSSION

The endocytic trafficking of several transmembrane proteins and ligands for receptors have been examined in the modified CHO cell line, TRVb-1 (McGraw *et al*., 1987; Dunn and Maxfield, 1992; Mukherjee *et al*., 1997; Ghosh *et al*., 1998; Mallet and Maxfield, 1999). A diagram of these endocytic trafficking pathways with our proposed itinerary for the CI-MPR is shown in Figure 10. Because the pool of CI-MPR mixes with the pool that cycles through late endosomes, it might have seemed most likely that the receptor would go by a direct route to late endosomes simply by staying in the sorting endosomes as they mature into late endosomes. This mechanism for delivery to late endosomes by retention in sorting endosomes was observed for furin (Mallet and Maxfield, 1999). However, pulse-chase experiments comparing internalized anti-bCI-MPR antibodies with endocytosed transferrin (which follows the recycling pathway) and LDL (which is retained in sorting endosomes as they mature into late endosomes) show clearly that nearly all the internalized

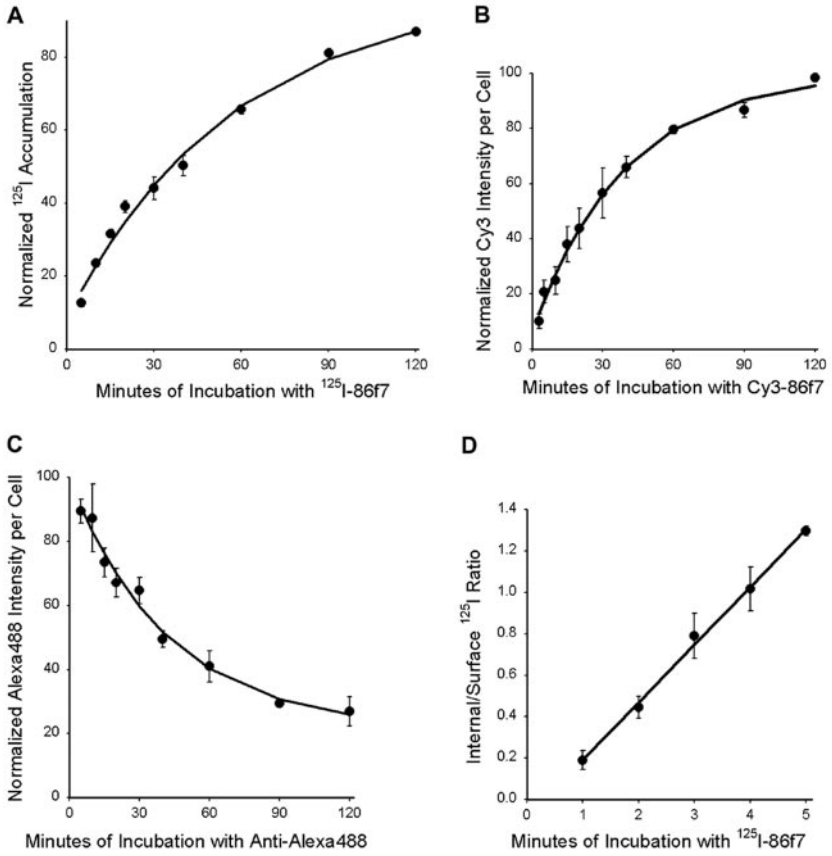

Figure 8. Kinetics of externalization and internalization of chimeric MPR. (A) Cells were incubated for 5, 10, 15, 20, 30, 45, 60, 90, and 120 min with 5 μg/ml ^{125}I-anti-bCI-MPR. Cells were washed with medium and dissolved in 0.1% SDS + 0.1 M NaOH. Solutes were collected and radioactivity determined using a gamma counter. Nonspecific binding to TRVb-1 cells not expressing the recombinant receptor was subtracted from the data. Data were fitted to a monoexponential increase. (B) Cells were incubated for 5, 10, 15, 20, 30, 45, 60, 90, and 120 min with 5 μg/ml Cy3-anti-bCI-MPR. Cells were washed, fixed, and imaged by epifluorescence microscopy, imaging 10 fields per time point. Data were fitted to a monoexponential increase. (C) Cells were incubated for 60 min with 5 μg/ml Alexa488-anti-bCI-MPR, and then washed and chased for 5, 10, 15, 20, 30, 45, 60, 90, and 120 min with 10 μg/ml anti-Alexa488. Cells were washed, fixed, and imaged by epifluorescence microscopy, imaging 10 fields per time point. Data were fitted to a monoexponential decline. (D) Cells received 5 μg/ml ^{125}I-anti-bCI-MPR for 1, 2, 3, 4, and 5 min at 37°C. Cells were immediately placed on ice and rapidly washed with cold buffer. Surface-bound ^{125}I was removed by 2 × 10-min incubations at pH 2 at 4°C. Internalized ^{125}I was recovered by dissolution in 0.1% SDS + 0.1 M NaOH. Shown is the ratio of internal to surface-bound counts as a function of time. Data were fitted to a straight line; the slope gives the internalization rate. For each experiment, time points were taken in triplicate. For all panels, data are the averages of three independent experiments. Error bars are SEs of the mean.

CI-MPR initially follows the endocytic recycling route (Figures 3 and 4); almost none of the internalized anti-bCI-MPR antibodies remains with cointernalized LDL after a 10-min chase (Figure 6). The transit of CI-MPR through the ERC was further confirmed by examining the effects of expressing a mutant form of the ERC-associated EH-domain protein, mRme-1. The G429R point mutant of mRme-1 was shown previously to slow the exit of both Tf and TGN38 from the ERC (Lin *et al.*, 2001). Expression of this mutant mRme-1 slowed the exit of chimeric CI-MPR from the ERC (Figure 5) and led to an ~40% decrease in the uptake of CI-MPR (Table 1). These results indicate that most CI-MPR passes through the ERC after internalization, and slowing exit from the ERC leads to an overall decrease in surface expression of CI-MPR. At steady state, only a small fraction of CI-MPR is associated with the ERC (Figures 1G and 2) because the receptor is removed rapidly from this compartment (Figures 3 and 4).

Table 2. Summary of quantitative characterizations of MPR trafficking

Parameter	Value	No. of experiments
Internalization rate (^{125}I-Ab uptake)	0.279 min^{-1} $t_{1/2}$ = 2.5 min	3
Externalization rate (^{125}I-Ab uptake)	0.0174 min^{-1} $t_{1/2}$ = 40 min	3
Externalization rate (Cy3-Ab uptake)	0.0255 min^{-1} $t_{1/2}$ = 27 min	3
Externalization rate (Ax488-Ab quench)	0.0237 min^{-1} $t_{1/2}$ = 29 min	3
Endocytic recycling rate (Ax488-Ab quench)	0.125 min^{-1} $t_{1/2}$ = 5.6 min	3
Expression level	6 × 10^5 copies per cell	3
% on plasma membrane (^{125}I-Ab uptake)	11%	3
% rapidly recycled	84%	3

Ab, antibody.

The CI-MPR has been detected previously in early and recycling endosomal fractions in rat liver (Runquist and Havel, 1991), and GFP-CI-MPR was found in transferrin-containing endosomes (Waguri *et al.*, 2003). In HepG2 human hepatoma cells a significant fraction of surface-iodinated ^{125}I-MPR remained associated with a Tf-containing compartment even after 45-min chase (van Weert *et al.*, 1995).

The detailed pathway followed by the fraction of CI-MPR that does not return to the cell surface is less clear, although it eventually distributes among late endosomes and a juxtanuclear distribution that includes the TGN. The pathway that is most consistent with our data is that some of the CI-MPR traffics from the ERC to the TGN, as has been observed for TGN38 (Ghosh *et al.*, 1998). This is suggested by the rapid transfer of internalized anti-bCI-MPR antibody from the ERC to a juxta-nuclear compartment that lacks transferrin and resembles the TGN (Figure 4). However, we cannot exclude the possibility of transport of CI-MPR from the ERC to a late endosome compartment followed by delivery to the TGN. As seen in Figure 3, although the majority of the CI-MPRs in the center of the cell are colocalized with

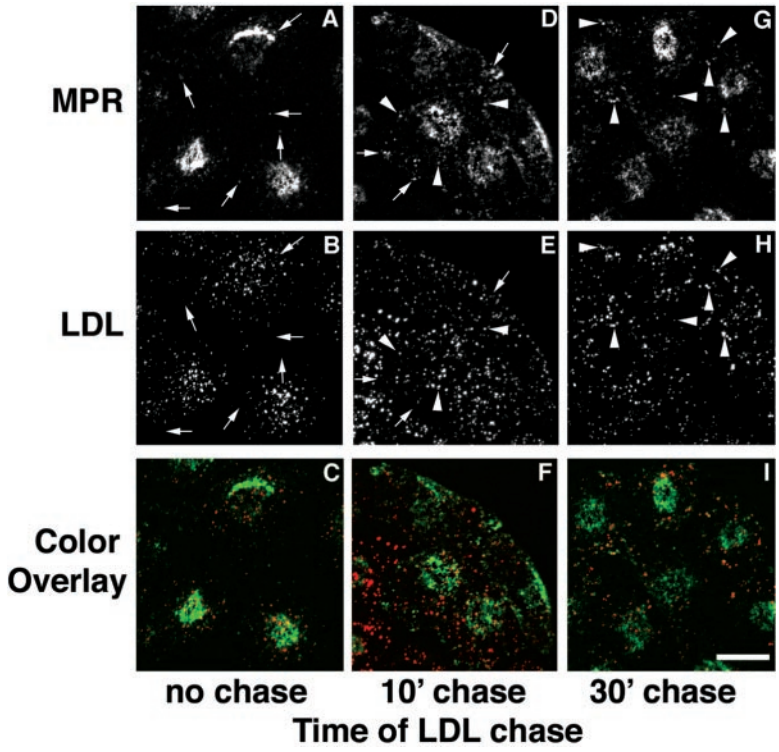

Figure 9. Chimeric CI-MPR appears in LDL-labeled late endosomes at a late stage in its endocytic trafficking. The cells were incubated with 5 μg/ml Alexa488-anti-bCI-MPR for 30 min followed by a 90-min chase. At the end of the chase, the cells were incubated for 5 min with 20 μg/ml DiI-LDL, washed, and fixed immediately (A–C) or chased for 10 (D–F) or 30 min (G–I) before fixation, such that for all samples the anti-MPR was chased for 90 min. In C, F, and I, internalized anti-bCI-MPR is colored green and LDL is colored red. Arrows in A and B indicate anti-bCI-MPR-labeled spots that do not label with LDL. Arrows in A, B, D, and E indicate nonoverlapping spots, and arrowheads in D, E, G, and H indicate double-labeled spots. Most CI-MPR is detected in a pericentriolar distribution, and the images have been enhanced to emphasize the dimmer punctate MPR labeling. Confocal Z-series projections are shown. Bars, 10 μm.

either Tf or TGN38, a minor population of CI-MPR showed no colocalization with either of these marker proteins. As expected based on numerous previous studies (Goda and Pfeffer, 1988; Griffiths *et al*., 1988; Dahms *et al*., 1989; Kornfeld, 1989), we did see some of the internalized anti-bCI-MPR antibodies in late endosomes that contained internalized LDL at longer chase times (Figure 9). At steady state, we found limited overlap of CI-MPR with the late endosome marker dextran (Figure 1F).

The relatively small fraction of the CI-MPR in late endosomes and its trafficking through the ERC were surprising because the function of the receptor is to deliver enzymes from the TGN or the external medium to late endosomes and lysosomes. However, the distribution and transport of

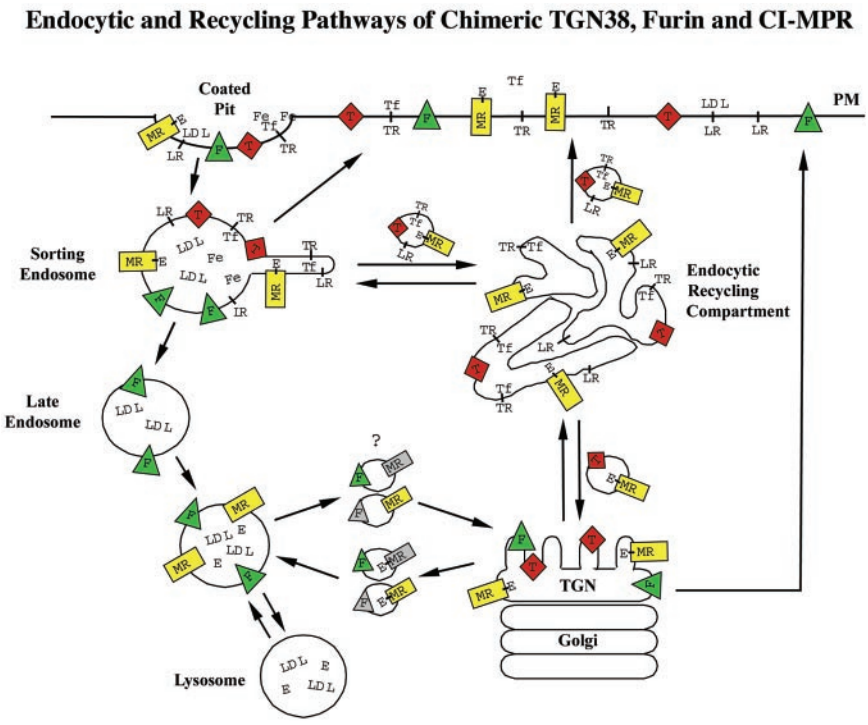

Figure 10. Schematic model of CI-MPR trafficking in CHO cells. The model compares the postendocytic itineraries of the CI-MPR (MR) and its enzyme ligands (E) with the transferrin receptor (TR), transferrin (Tf) with or without iron (Fe), the LDL receptor (LR), LDL, furin (F), and TGN38 (T). All of the membrane proteins concentrate into clathrin-coated pits, and the initial delivery site is sorting endosomes. Most of the membrane proteins, including CI-MPR, rapidly exit this compartment and are either returned directly to the plasma membrane (PM) or are transported to the ERC. Furin is retained in the sorting endosome as it begins to mature into a late endosome, and furin reaches the Golgi via the late endosomes. From the ERC, essentially all of the transferrin receptors recycle to the cell surface, and ~85% of the internalized TGN38 and CI-MPR also return to the cell surface. The remaining TGN38 and CI-MPR are delivered to the *trans*-Golgi. The CI-MPR traffics from the *trans*-Golgi to late endosomes, where the enzyme ligands dissociate as a consequence of exposure to a sufficiently acidic pH. Furin and the empty CI-MPR return to the *trans*-Golgi. It is not known if furin and CI-MPR share the same transport vesicle as they shuttle between late endosomes and the *trans*-Golgi. A portion of all of the molecules in the *trans*-Golgi is delivered to the cell surface.

CI-MPR in our studies were consistent with the previous observations of a transient appearance of internalized CI-MPR in endosomes carrying epidermal growth factor and its receptor and an overall deficiency of the receptor in multivesicular bodies (Hirst *et al*., 1998). The vesicles that contain endocytosed cargo and the CI-MPR may be those that are receiving hydrolytic enzymes, or this may represent receptor that is destined for degradation. If retrieval of most CI-MPR out of these endosomes is rapid, little should be found in late endosomes at any given time.

Late endosomes show a range of morphologies and enrichment for different markers (Kleijmeer *et al*., 1997). Preferential delivery of CI-MPR to a subset of late endosomes might contribute to the relatively small number of cargo-containing endosomes that also contain detectable CI-MPR in TRVb-1 cells. The abundance of different types of late endosomes and the kinetics of delivery and removal from these endosomes could vary among cell types, explaining the different degrees of enrichment of the CI-MPR in compartments of different cell types.

It is difficult to say with precision how the complex itinerary of endocytosed CI-MPR relates to the fate of enzymes that are bound to the receptor and internalized. The $t_{1/2}$ of CI-MPR internalization is 2.5 min, and after a short pulse ~80% of the internalized receptor is externalized with a $t_{1/2}$ of 5.6 min. Previously, it was found that the $t_{1/2}$ for acidification-dependent ligand dissociation from the CI-MPR is 11 min (Borden *et al*., 1990). An unresolved question is precisely where the dissociation occurs. The pH of sorting endosomes is ~5.9–6.2 (Presley *et al*., 1993), and the midpoint for the pH dependence of CI-MPR binding is around pH 5.8 (Borden *et al*., 1990). It is possible that the pH of the sorting endosomes fluctuates below 5.8. It is also possible that some dissociation occurs at slightly higher pH values under the conditions in sorting endosomes. If the efficiency of ligand dissociation during each pass through the sorting endosomes was ~40%, it could account for the dissociation kinetics reported in our previous study (Borden *et al*., 1990). Some enzymes could remain bound to the receptors as they pass through the ERC, which has a pH of 6.4 (Yamashiro *et al*., 1984), and then dissociate when the receptors reach the late endosomes.

In addition to delivery from the sorting endosomes into the ERC, CI-MPRs may also enter the ERC from the Golgi. A recent study showed that a significant amount of GFP-CI-MPR leaving the TGN was delivered to peripheral tubular endosomes that contain Tf internalized from the cell surface in HeLa cells (Waguri *et al*., 2003). The ERC in HeLa cells is composed of tubular endosomal structures distributed throughout the cell (Lin *et al*., 2002), and similar structures are seen in the closely related HEp2 cell line (Ghosh *et al*., 1994). Because Alexa594-Tf was incubated with HeLa cells for 10–15 min in the study of GFP-CI-MPR transport out of the TGN (Waguri *et al*., 2003), it is likely that the Tf-positive tubular structures into which the CI-MPRs were delivered are mostly ERC elements and not sorting endosomes. A high fraction of the CI-MPR in the ERC recycles to the cell surface (Figure 7). This apparently futile recycling and inefficient delivery to the TGN was also observed after internalization of TGN38 (Ghosh *et al*., 1998).

The present study of CI-MPR endocytic trafficking, together with our previous studies on the internalization pathways of TGN38 (Ghosh *et al*., 1998) and furin (Mallet *et al*., 1999), reveal the distinct itineraries of three known proteins that traffic between the plasma membrane and TGN. These studies will provide the basis for future studies to explore the regulatory elements involved in the various steps of these complex and interconnected transport pathways.

ACKNOWLEDGMENTS

We thank Peter Lobel for the chimeric CI-MPR construct and extensive advice and guidance. We thank many other investigators (acknowledged in MATERIALS AND METHODS) for their kind gifts of antibodies and reagents. We also thank Dr. Timothy McGraw and members of the Maxfield and McGraw laboratories for critical input during these studies. We thank Dr. Lori Tortorella for critical reading of the manuscript. We thank Dr. Zahra Mamdouh for preparing and providing labeled LDL and Rose Soe for technical assistance. This work was supported by National Institutes of Health grant DK27083. During the initial stages of this study, W.G.M. was supported by a postdoctoral fellowship from the Pharmaceutical Research and Manufacturers of America Foundation.

REFERENCES

Borden, L.A., Einstein, R., Gabel, C.A., and Maxfield, F.R. (1990). Acidification-dependent dissociation of endocytosed insulin precedes that of endocytosed proteins bearing the mannose 6-phosphate recognition marker. J. Biol. Chem. *265*, 8497–8504.

Bosshart, H., Humphrey, J., Deignan, E., Davidson, J., Drazba, J., Yuan, L., Oorschot, V., Peters, P.J., and Bonifacino, J.S. (1994). The cytoplasmic domain mediates localization of furin to the *trans*-Golgi network en route to the endosomal/lysosomal system. J. Cell Biol. *126*, 1157–1172.

Chen, H.J., Remmler, J., Delaney, J.C., Messner, D.J., and Lobel, P. (1993). Mutational analysis of the cation-independent mannose 6-phosphate/insulin-like growth factor II receptor. J. Cell Biol. *268*, 22338–22346.

Chen, H.J., Yuan, J., and Lobel, P. (1997). Systematic mutational analysis of the cation-independent mannose 6-phosphate/insulin-like growth factor II receptor cytoplasmic domain. J. Biol. Chem. *272*, 7003–7012.

Dahms, N.M., Lobel, P., and Kornfeld, S. (1989). Mannose 6-phosphate receptors and lysosomal enzyme targeting. J. Biol. Chem. *264*, 12115–12118.

Dell'Angelica, E.C., Klumperman, J., Stoorvogel, W., and Bonifacino, J.S. (1998). Association of the AP-3 adaptor complex with clathrin. Science *280*, 431–434.

Doray, B., Ghosh, P., Griffith, J., Geuze, H.J., and Kornfeld, S. (2002). Cooperation of GGAs and AP-1 in packaging MPRs at the trans-Golgi network. Science *297*, 1700–1703.

Drake, M.T., Zhu, Y., and Kornfeld, S. (2000). The assembly of AP-3 adaptor complex-containing clathrin-coated vesicles on synthetic liposomes. Mol. Biol. Cell *11*, 3723–3736.

Duden, R., Griffiths, G., Frank, R., Argos, P., and Kreis, T. (1991). Beta-COP, a 110 kD protein associated with non-clathrin-coated vesicles and the Golgi complex, shows homology to beta-adaptin. Cell *64*, 649–665.

Duncan, J.R., and Kornfeld, S. (1988). Intracellular movement of two mannose 6-phosphate receptors: return to the Golgi apparatus. J. Cell Biol. *106*, 617–628.

Dunn, K.W., and Maxfield, F.R. (1992). Delivery of ligands from sorting endosomes to late endosomes occurs by maturation of sorting endosomes. J. Cell Biol. *117*, 301–310.

Geuze, H.J., Slot, J.W., Strous, G.J.A.M., Hasilik, A., and von Figura, K. (1984). Ultrastructural localization of the mannose 6-phosphate receptor in rat liver. J. Cell Biol. *98*, 2047–2054.

Ghosh, P., and Kornfeld, S. (2003). Phosphorylation-induced conformational changes regulate GGAs 1 and 3 function at the trans-Golgi network. J. Biol. Chem. *278*, 14543–14549.

Ghosh, R., Gelman, D., and Maxfield, F. (1994). Quantification of low density lipoprotein and transferrin endocytic sorting HEp2 cells using confocal microscopy. J. Cell Sci. *107*, 2177–2189.

Ghosh, R.N., Mallet, W.G., Soe, T.T., McGraw, T.E., and Maxfield, F.R. (1998). An endocytosed TGN38 chimeric protein is delivered to the TGN after trafficking through the endocytic recycling compartment in CHO cells. J. Cell Biol. *142*, 923–936.

Goda, Y., and Pfeffer, S.R. (1988). Selective recycling of the mannose 6-phosphate/IGF-II receptor to the *trans*-Golgi network in vitro. Cell *55*, 309–320.

Griffiths, G., Hoflack, B., Simons, K., Mellman, I., and Kornfeld, S. (1988). The mannose 6-phosphate receptor and the biogenesis of lysosomes. Cell *52*, 329–341.

Hao, M., and Maxfield, F.R. (2000). Characterization of rapid membrane internalization and recycling. J. Biol. Chem. *275*, 15279–15286.

Hinners, I., and Tooze, S. (2003). Changing directions: clathrin-mediated transport between the Golgi and endosomes [In Process Citation]. J. Cell Sci. *116*, 763–771.

Hirst, J., Futter, C., and Hopkins, C. (1998). The kinetics of mannose 6-phosphate receptor trafficking in the endocytic pathway in HEp-2 cells: the receptor enters and rapidly leaves multivesicular endosomes without accumulating in a prelysosomal compartment. Mol. Biol. Cell *9*, 809–816.

Hirst, J., and Robinson, M.S. (1998). Clathrin and adaptors. Biochim. Biophys. Acta *1404*, 173–193.

Hopkins, C.R., and Trowbridge, I.S. (1983). Internalization and processing of transferrin and the transferrin receptor in human carcinoma A431 cells. J. Cell Biol. *97*, 508–521.

Humphrey, J.S., Peters, P.J., Yuan, L.C., and Bonifacino, J.S. (1993). Localization of TGN38 to the *trans*-Golgi network: involvement of a cytoplasmic tyrosine-containing sequence. J. Cell Biol. *120*, 1123–1135.

Jin, M., Sahagian, G.G., and Snider, M.D. (1989). Transport of surface mannose 6-phosphate receptor to the Golgi complex in cultured human cells. J. Biol. Chem. *264*, 7675–7680.

Kleijmeer, M.J., Morkowski, S., Griffith, J.M., Rudensky, A.Y., and Geuze, H.J. (1997). Major histocompatibility complex class II compartments in human and mouse B lymphoblasts represent conventional endocytic compartments. J. Cell Biol. *139*, 639–649.

Kobayashi, T., Beuchat, M., Lindsay, M., Frias, S., Palmiter, R., Sakuraba, H., Parton, R., and Gruenberg, J. (1999). Late endosomal membranes rich in lysobisphosphatidic acid regulate cholesterol transport. Nat. Cell Biol. *1*, 113–118.

Kornfeld, S. (1989). The biogenesis of lysosomes. Annu. Rev. Cell Biol. *5*, 483–525.

Le Borgne, R., Alconada, A., Bauer, U., and Hoflack, B. (1998). The mammalian AP-3 adaptor-like complex mediates the intracellular transport of lysosomal membrane glycoproteins. J. Biol. Chem. *273*, 29451–29461.

Lin, S.X., Gundersen, G., and Maxfield, F. (2002). Export from pericentriolar endocytic recycling compartment to cell surface depends on stable, detyrosinated (glu) microtubules and kinesin. Mol. Biol. Cell *13*, 96–109.

Lin, S.X., Grant, B., Hirsh, D., and Maxfield, F.R. (2001). Rme-1 regulates the distribution and function of the endocytic recycling compartment in mammalian cells. Nat. Cell Biol. *3*, 567–572.

Lippincott-Schwartz, J., and Fambrough, D.M. (1987). Cycling of the integral membrane glycoprotein, LEP100, between plasma membrane and lysosomes: kinetic and morphological analysis. Cell *49*, 669–677.

Luzio, J.P., Brake, B., Banting, G., Howell, K.E., Braghetta, P., and Stanley, K.K. (1990). Identification, sequencing and expression of an integral membrane protein of the *trans*-Golgi network (TGN38). Biochem. J. *270*, 97–102.

Mallet, W.G., and Maxfield, F.R. (1999). Chimeric forms of furin and TGN38 are transported from the plasma membrane to the TGN via distinct endosomal pathways. J. Cell Biol. *146*, 345–359.

Mayor, S., Presley, J.F., and Maxfield, F.R. (1993). Sorting of membrane components from endosomes and subsequent recycling to the cell surface occurs by a bulk flow process. J. Cell Biol. *121*, 1257–1269.

McGraw, T.E., Greenfield, L., and Maxfield, F.R. (1987). Functional expression of the human transferrin receptor cDNA in Chinese hamster ovary cells deficient in endogenous transferrin receptor. J. Cell Biol. *105*, 207–214.

McGraw, T.E., and Maxfield, F.R. (1990). Human transferrin receptor internalization is partially dependent upon an aromatic amino acid on the cytoplasmic domain. Cell Reg. *1*, 369–377.

Messner, D.J. (1993). The mannose receptor and the cation-dependent form of mannose 6-phosphate receptor have overlapping cellular and subcellular distributions in liver. Arch. Biochem. Biophys. *306*, 391–401.

Misumi, Y., Oda, K., Fujiwara, T., Takami, N., Tashiro, K., and Ikehara, Y. (1991). Functional expression of furin demonstrating its intracellular localization and endoprotease activity for processing of proalbumin and complement pro-C3. J. Biol. Chem. *266*, 16954–16959.

Miwako, I., Yamamoto, A., Kitamura, T., Nagayama, K., and Ohashi, M. (2001). Cholesterol requirement for cation-independent mannose 6-phosphate receptor exit from multivesicular late endosomes to the Golgi. J. Cell Sci. *114*, 1765–1776.

Mukherjee, S.M., Ghosh, R.N., and Maxfield, F.R. (1997). Endocytosis. Physiol. Rev. *77*, 759–803.

Ohashi, M., Miwako, I., Yamamoto, A., and Nagayama, K. (2000). Arrested maturing multivesicular endosomes observed in a Chinese hamster ovary cell mutant, LEX2, isolated by repeated flow-cytometric cell sorting. J. Cell Sci. *113*, 2187–2205.

Pagano, R.E., Sepanski, M.A., and Martin, O.C. (1989). Molecular trapping of a fluorescent ceramide analogue at the Golgi apparatus of fixed cells: interaction with endogenous lipids provides a *trans*-Golgi marker for both light and electron microscopy. J. Cell Biol. *109*, 2067–2079.

Pitas, R.E., Innerarity, T.L., Weinstein, J.N., and Mahley, R.W. (1981). Acetoacetylated lipoproteins used to distinguish fibroblasts from macrophages *in vitro* by fluorescence microscopy. Arteriosclerosis *1*, 177–185.

Ponnambalam, S., Rabouille, C., Luzio, J.P., Nilsson, T., and Warren, G. (1994). The TGN38 glycoprotein contains two non-overlapping signals that mediate localization to the *trans*-Golgi network. J. Cell Biol. *125*, 253–268.

Presley, J., Mayor, S., Dunn, K., Johnson, L., McGraw, T., and Maxfield, F. (1993). The End2 mutation in CHO cells slows the exit of transferrin receptors from the recycling compartment but bulk membrane recycling is unaffected. J. Cell Biol. *122*, 1231–1241.

Press, B., Feng, Y., Hoflack, B., and Wandinger-Ness, A. (1998). Mutant Rab7 causes the accumulation of cathepsin D and cation-independent mannose 6-phosphate receptor in an early endocytic compartment. J. Cell Biol. *140*, 1075–1089.

Puertollano, R., Aguilar, R.C., Gorshkova, I., Crouch, R.J., and Bonifacino, J.S. (2001). Sorting of mannose 6-phosphate receptors mediated by the GGAs. Science *292*, 1712–1716.

Runquist, E., and Havel, R. (1991). Acid hydrolases in early and late endosome fractions from rat liver. J. Biol. Chem. *266*, 22557–22563.

Sahagian, G., and Neufeld, E. (1983). Biosynthesis and turnover of the mannose 6-phosphate receptor in cultured Chinese hamster ovary cells. J. Biol. Chem. *258*, 7121–7128.

Salzman, N.H., and Maxfield, F.R. (1989). Fusion accessibility of endocytic compartments along the recycling and lysosomal endocytic pathways in intact cells. J. Cell Biol. *109*, 2097–2104.

Traub, L., Ostrom, J., and Kornfeld, S. (1993). Biochemical dissection of AP-1 recruitment onto Golgi membranes. J. Cell Biol. *123*, 561–573.

Uthayakumar, S., and Granger, B. (1995). Cell surface accumulation of overexpressed hamster lysosomal membrane glycoproteins. Cell. Mol. Biol. Res. *41*, 405–420.

van Weert, A., Dunn, K., Gueze, H., Maxfield, F., and Stoorvogel, W. (1995). Transport from late endosomes to lysosomes, but not sorting of integral membrane proteins in endosomes, depends on the vacuolar proton pump. J. Cell Biol. *130*, 821–834.

Voorhees, P., Deignan, E., van Donselaar, E., Humphrey, J., Marks, M.S., Peters, P.J., and Bonifacino, J.S. (1995). An acidic sequence within the cytoplasmic domain of furin functions as a determinant of *trans*-Golgi network localization and internalization from the cell surface. EMBO J. *14*, 4961–4975.

Waguri, S., Dewitte, F., Le, B.R., Rouille, Y., Uchiyama, Y., Dubremetz, J., and Hoflack, B. (2003). Visualization of TGN to endosome trafficking through fluorescently labeled MPR and AP-1 in living cells. Mol. Biol. Cell *14*, 142–155.

Wilde, A., Reaves, B., and Banting, G. (1992). Epitope mapping of two isoforms of a trans Golgi network specific integral membrane protein TGN38/41. FEBS Lett. *313*, 235–238.

Willingham, M.C., Pastan, I.H., and Sahagian, G.G. (1983). Ultrastructural immunocytochemical localization of the phosphomannosyl receptor in Chinese hamster ovary (CHO) cells. J. Histochem. Cytochem. *31*, 1–11.

Yamashiro, D.J., Borden, L.A., and Maxfield, F.R. (1989). Kinetics of alpha 2-macroglobulin endocytosis and degradation in mutant and wild-type Chinese hamster ovary cells. J. Cell Physiol. *139*, 377–382.

Yamashiro, D.J., Tycko, B., Fluss, S.R., and Maxfield, F.R. (1984). Segregation of transferrin to a mildly acidic (pH 6.5) para-Golgi compartment in the recycling pathway. Cell *37*, 789–800.

Zhu, Y., Doray, B., Poussu, A., Lehto, V.P., and Kornfeld, S. (2001). Binding of GGA2 to the lysosomal enzyme sorting motif of the mannose 6-phosphate receptor. Science *292*, 1716–1718.